Influence of small-cluster mobility on the island formation in molecular beam epitaxy

Sang Bub Lee and Bikash C. Gupta
Department of Physics, Kyungpook National University, Taegu, 702-701 Korea
(Received 5 April 2000)

We study by Monte Carlo simulation submonolayer thin film growth during molecular beam epitaxy. We carry out a variety of simulations, both with and without inclusion of the small-cluster mobility and the detachment of one-bond adatoms from island edges, using the solid-on-solid model with the full excluded volume of adatoms. We find that the small-cluster mobility appears to influence the scaling relation of the island density and the scaling functions of the island size distributions. The scaling exponent χ defined by the island density N via $N \sim F^{\chi}$, F being the deposition flux, is found to vary, as the substrate temperature increases, from $\chi = \frac{1}{3}$ to $\chi = \frac{2}{5}$ if the detachment of adatoms is disallowed and to a value beyond $\frac{2}{5}$ if detachment is allowed. It appears from these results that there exists an intermediate region in which rate equation analysis with small-cluster mobility is adequate before the onset of $i > 1$ behavior. We also study the influences of edge diffusion, small-cluster mobility, and adatom detachment on the scaling function.

I. INTRODUCTION

Molecular beam epitaxy (MBE) is an important technological process for fabricating nanostructures of high-purity crystals.[1–3] The fundamental physical processes in MBE involve nucleation by two or more atoms, aggregation of adatoms on island edges, and coalescence of two or more islands. These processes lead to the formation of a distribution of islands with various sizes.

At low temperature, adatoms diffuse slowly (with low hopping rate) on a substrate, and clusters of two or more atoms are immobile and become stable. The diffusion rate of adatoms (monomers) depends on the temperature via $D = D_0 \exp(-E_{d1}/k_B T)$, E_{d1} being the diffusion barrier for a monomer and D_0 the free hopping rate per atom. An island grows in a similar way as diffusion-limited aggregation (DLA) and shows a fractal nature with a fractal dimension similar to that of DLA, i.e., $d_F \simeq 1.7$.[4–6] As the temperature increases, monomers diffuse with a higher hopping rate and adatoms on an island edge slip along the edge, yielding edge diffusion. When an adatom arrives at a kink site at which more lateral bonds can be formed, it will become immobile. It is known that such edge diffusion yields a geometrical phase transition of the island morphology from fractal to compact structures. For such submonolayer nucleation and growth of islands during deposition, the power-law behavior of the island density with deposition flux and the scaling of the island size distributions are of primary interest.

Classical rate equation analysis and the more recent development of dynamic scaling ideas have provided powerful tools for understanding the growth and aggregation processes in terms of the evolution of the cluster size distribution. In the early stage of deposition, the density of islands N increases as[7]

$$N \sim (D/F)^{-\chi} \exp[\beta E_i/(i+2)], \tag{1}$$

for fixed coverage θ $(=Ft$, F being the deposition flux), where $\beta = 1/k_B T$ and $\chi = i/(i+2)$.[8] The critical island size i is the size of clusters one atom smaller than the size of the smallest stable islands and E_i is the dissociation energy of clusters of size i.

The exponent χ may be determined experimentally by studying the variation of N as a function of the substrate temperature and the deposition flux, using various techniques such as scanning tunneling microscopy, transmission electron microscopy, and high-resolution diffraction and scattering. Once χ is known, the prefactor D_0 and the diffusion barrier E_{d1} can be determined from the constant $N(D/F)^{\chi}$ for various values of the substrate temperature. Thus, knowledge of the scaling behavior of the island density and the island size distribution enables one to determine important physical quantities in epitaxial growth. A typical value of D_0 for metal-on-metal deposition is known to be of the order of 10^{13} (hops per atom per second).

During the aggregation process, on the other hand, the island density remains nearly constant, while the mean island size increases. The self-similar island size distribution in time during such processes yields the density of islands of size s, N_s, scaling as

$$N_s \sim \frac{t}{S^2} f(s/S), \tag{2}$$

where S and t are, respectively, the mean size of islands and the evolution time. This dynamic scaling relation has been used by Family and Meakin[9] to study the size distribution of droplets of liquid and has now become the standard mathematical tool for the study of growing surfaces.[9–11] A great deal of effort has also been devoted to the study of the analytical form of the scaling functions.[11–14]

As the temperature increases further, clusters of small size such as dimers and trimers begin to diffuse. The influence of small-cluster mobility has recently been investigated with a rather simple model of ''point'' islands or ''zero-size'' islands.[15,16] Classical mean-field rate equation analysis allows us to predict that the island density scales with deposition flux F as[17]

$$N \sim (F/D)^{2/5} \exp[\beta(E_{d1}+E_{d2})/5] \tag{3}$$

if each monomer hops with the rate $D=D_0 e^{-\beta E_{d1}}$ and each dimer with $D_2=D_0 e^{-\beta E_{d2}}$, but trimers and larger clusters are immobile.

At sufficiently high temperature, where adatom detachment becomes operative from the island edges, dimers may dissociate into two monomers before they diffuse large distances, implying that monomer diffusion dominates dimer mobility. The scaling relation in Eq. (1) thus holds for some $i>1$ and the exponent χ increases from $\chi=\frac{1}{3}$ to $\chi=\frac{1}{2}$ or even larger. Earlier work[15,16] focused on whether or not there is an intermediate region in which the scaling relation in Eq. (3) holds before such a transition occurs. Liu, Bonig, and Metiu[15] argued that mobilities of small clusters significantly affect the island density before the transition from $i=1$ behavior to $i=2$ behavior occurs. They emphasized that the modified scaling relation in Eq. (3) should be considered in the analysis of experimental data. On the other hand, Bartelt *et al.*[16] claimed that dimer hopping dominating dissociation is not sufficient to guarantee such a scaling region before the onset of $i>1$ behavior. In both studies, however, it was assumed that two monomers on the same site form a dimer. Although the authors claim that such an assumption is valid in the submonolayer regime of $\theta \leqslant 0.15$, we argue that the model is not appropriate to simulate epitaxial growth for the coverages used.

In this work, we study, by kinetic Monte Carlo simulation based on the solid-on-solid model, the influences of small-cluster mobility and adatom detachment on island formation, using the full excluded volume of adatoms. We focus on the density profiles of monomers and islands, on the scaling exponent χ characterizing the island density versus the deposition flux for various substrate temperatures, and on the scaling function of the island size distributions. We carry out a variety of simulations both with and without dimer and trimer mobilities and adatom detachment and calculate the densities of monomers and islands versus the coverage and the deposition flux. The island size distribution and scaling function are also calculated.

This paper is organized as follows. In Sec. II, we review the rate equation analyses with and without small-cluster mobility and present the scaling relations of the monomer and dimer densities. In Sec. III, we present the details of our simulation procedure, and in Sec. IV, we present the results and discussion. The summary and conclusions are presented in Sec. V.

II. RATE EQUATION ANALYSIS RECONSIDERED

Ignoring small-cluster mobility and dissociation of adatoms, the rate equations of the monomer density $N_1(t)$ and the density of islands of size s, $N_s(t)$, can be written as

$$\frac{dN_1}{dt} = F - 2K_1 N_1^2 - \sum_{s \geqslant 2} K_s N_1 N_s, \tag{4}$$

$$\frac{dN_s}{dt} = N_1 (K_{s-1} N_{s-1} - K_s N_s), \tag{5}$$

in the early stage of deposition, where K_s corresponds to the cross section for the capture of monomers by islands of size s, i.e., the rate of adsorption of monomers by islands. It is clear that K_s is proportional to the diffusion constant of monomers and the surface area of islands of size s, i.e., $K_s \sim D s^p$, with $p=1/d_f$ for fractal islands of fractal dimension d_f and $p=1/2$ for compact islands. Dividing both equations by F and taking a sum over all islands, one can recast the equations in terms of the coverage:

$$\frac{dN_1}{d\theta} = 1 - 2RN_1^2 - R\sum_{s \geqslant 2} s^p N_1 N_s, \tag{6}$$

$$\frac{dN}{d\theta} = RN_1^2 \tag{7}$$

with $R=D/F$. The solution of these equations is known to be readily obtained, for the point island model of $p=0$, as $N_1 \sim \theta$ and $N \sim R\theta^3$ at early time, and $N_1 \sim R^{-2/3}\theta^{-1/3}$ and $N \sim R^{-1/3}\theta^{1/3}$ at late time, and, for the compact island model, as $N_1 \sim R^{-3/4}\theta^{-1/2}$ and $N \sim R^{-1/2}(\ln \theta)$ at late time.[11]

For processes including dimer mobilities, the rate equations are modified as

$$\frac{dN_1}{dt} = F - KDN_1 N - K(D+D_2)N_1 N_2 - 2KDN_1^2 \simeq F - KDN_1 N, \tag{8}$$

$$\frac{dN_2}{dt} = KDN_1^2 - K(D+D_2)N_1 N_2 - KD_2 N_2 N - 2KD_2 N_2^2 \simeq KDN_1^2 - KD_2 N_2 N, \tag{9}$$

$$\frac{dN_s}{dt} = KDN_1(N_{s-1}-N_s) + KD_2 N_2 (N_{s-2}-N_s) \simeq KDN_1(N_{s-1}-N_s), \quad (s \geqslant 3), \tag{10}$$

where we assumed $D \gg D_2$ and $N_1, N_2 \ll N$ at high temperature, where small-cluster mobility is expected to be important. Using $N=\Sigma_{s \geqslant 3} N_s$ and the steady-state conditions of $dN_1/dt \simeq dN_2/dt \simeq 0$, one obtains Eq. (3) for island density and

$$N_1 \sim (F/D)^{3/5} \exp[-\beta(E_{d2}-4E_{d1})/5)], \tag{11}$$

$$N_2 \sim (F/D)^{4/5} \exp[2\beta(E_{d1}+E_{d2})/5] \tag{12}$$

for monomer and dimer densities.

III. MONTE CARLO SIMULATION

In the usual kinetic Monte Carlo simulations, adatoms are deposited with a flux F (atoms per second per area) on a flat substrate of a square lattice and diffuse along any one of the coordinate directions at each step until they encounter another adatom or an island. An adatom deposited on top of an existing island is also assumed to diffuse, with the same diffusion rate as a monomer on the substrate, until it encounters another adatom or a step edge. It may also hop down to a lower layer by normal diffusion. Such a walker, however, is not considered to be a monomer, but is rather assumed as a member of the underlying island. In this procedure, since our primary interest is to investigate island formation in the

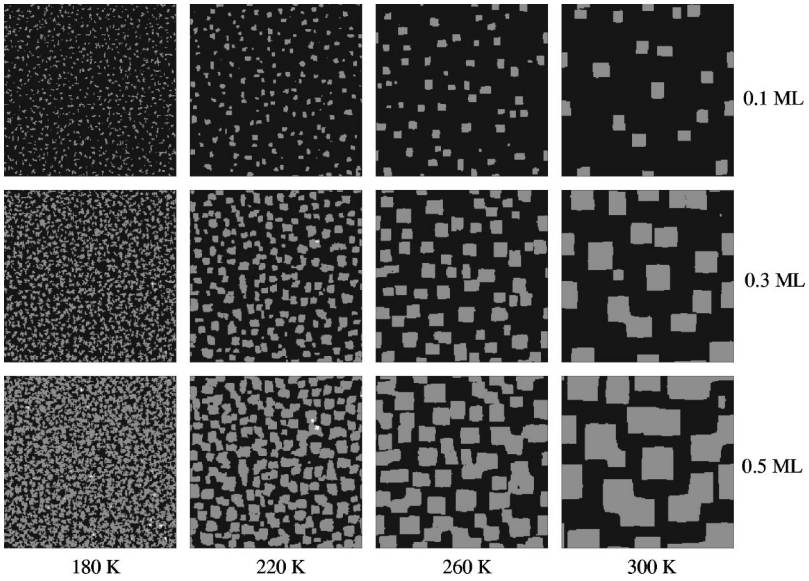

FIG. 1. Typical contour diagrams of the surface morphologies for the selected values of temperature and coverage.

early stage of deposition with a coverage less than 0.2 monolayer (ML), we ignore the Ernlich-Schwoebel barriers for interlayer transport at step edges. Despite this approximation, we believe that our model can be applied to higher coverages than those of earlier works.

Small clusters such as dimers and trimers are also assumed to diffuse with a hopping rate depending on the temperature and diffusion barriers. When an adatom on a substrate encounters another adatom, the two atoms form a dimer. When an adatom encounters an island of size s, it sticks on the island yielding an island of size $s+1$. Similarly, when a dimer encounters an island of size s, the island size becomes $s+2$. Atoms attached to island edges with one lateral bond may be dissociated from the islands (as well as diffusing along the edges of islands) and become diffusing monomers (i.e., walkers) at the cost of the dissociation energy of dimers.

At each simulation step, one of the following transition processes is selected: (a) *deposition* of adatoms on a site of the $L\times L$ square lattice with flux F, (b) *diffusion* of a monomer with the hopping rate $D=D_0e^{-E_{d1}/k_BT}$ (hops per second per adatom), (c) *edge diffusion* of adatoms on an island edge with the hopping rate $D_e=D_0e^{-E_e/k_BT}$, E_e being the potential barrier for edge diffusion, (d) *adatom detachment* from an island with the rate $D_{dis}=D_0e^{-E_{dis}/k_BT}$, E_{dis} being the dissociation barrier, (e) *diffusion of dimers* with the hopping rate $D_2=D_0e^{-E_{d2}/k_BT}$, and (f) *diffusion of trimers* with the hopping rate $D_3=D_0e^{-E_{d3}/k_BT}$.

Clusters of size larger than 3 are assumed to be immobile throughout the simulation, although they may be dissociated to smaller clusters by adatom detachment and become mobile. The transition probabilities are proportional to F, $N_1D_0e^{-E_{d1}/k_BT}$, $N_eD_0e^{-E_e/k_BT}$, $N_{dis}D_0e^{-E_{dis}/k_BT}$, $N_2D_0e^{-E_{d2}/k_BT}$, and $N_3D_0e^{-E_{d3}/k_BT}$, where N_1, N_e, N_{dis}, N_2, and N_3 are the numbers of transition candidates per site for each transition. The list of transition candidates was kept and updated throughout the simulations. The normalized transition probabilities can thus be readily obtained from the transition rates and the numbers of candidates for each transition.

The typical size of system we use in our simulations is $L=1000$ for all cases, except for calculations of the scaling function in Eq. (2), for which $L=512$ is used. Simulations are carried out irreversibly until the desired coverage is achieved. Once the desired coverage is reached, the cluster size distributions are calculated using the well-known cluster labeling algorithm.[18] The monomer density N_1, the dimer density N_2, the island density $N=\Sigma_{s\geqslant 3}N_s$, and the mean island size $S=\Sigma_{s\geqslant 3}sN_s/\Sigma_{s\geqslant 3}N_s$ are then readily determined from the knowledge of N_s.

IV. RESULTS

In most of our simulations, we use a prefactor of the diffusion constant $D_0=10^{13}$ and a deposition rate F_0 between 10^{-5} and an order of 10 depending on the substrate temperature, which varies between 160 and 360 K. The transition barriers used are $E_{d1}=0.4$ eV, $E_{dis}=0.72$ eV, $E_e=E_{d2}=0.5$ eV, and $E_{d3}=0.55$ eV, which are reasonable for metal-on-metal epitaxy such as Al/Al(111),[19] Pt/Pt(100),[20] and Fe/Cu(111).[21] Typical contour diagrams of the island morphologies for selected temperatures and coverages are shown in Fig. 1. For simulations without dissociation or small-cluster mobility (corresponding to the cases of $E_{dis}=\infty$ or $E_{d2}=E_{d3}=\infty$), we eliminate the corresponding processes from the simulation procedure.

In order to investigate the influence of dimer mobility, we calculate the monomer and island densities versus the coverage and the deposition flux for the following three models: (i) only monomers diffuse, (ii) monomers and dimers diffuse but adatom detachment is not allowed, and (iii) monomers and dimers diffuse and adatom detachment is allowed. In all three cases, edge diffusion is always allowed unless otherwise stated explicitly. We also carry out additional simulations with trimer mobility.

A. Monomer and island densities versus coverage

In order to observe the influence of small-cluster mobility on the monomer and island densities, we plot in Fig. 2 N_1 and N against the coverage, for two typical values of the substrate temperature, $T=240$ K and $T=300$ K. The solid

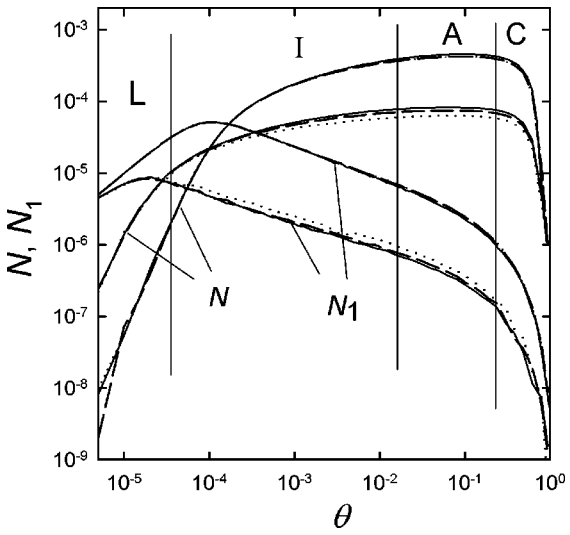

FIG. 2. Monomer and island densities versus the coverage for selected values of the substrate temperature. The upper sets are for $T=240$ K and the lower sets for $T=300$ K, and the solid lines are for model (i), the dashed lines for (ii), and the dotted lines for (iii). The density profile is divided into four different regions, indicated as L (low-coverage regime), I (intermediate regime), A (aggregation regime), and C (coalescence regime), details of which are described in the text.

lines are the data from the model (i), the dashed lines from (ii), and the dotted lines from (iii). The upper sets are for $T=240$ K and the lower sets for $T=300$ K. Although the correct definition of N should be $N=\Sigma_{s\geqslant 3}N_s$ for (ii) and (iii), we use $N=\Sigma_{s\geqslant 2}N_s$ for all models to enable us to directly compare the results of (ii) and (iii) with those of (i). (Note, however, that inclusion of dimers does not affect the result appreciably except in the low-coverage regime.)

For the low temperature of $T=240$ K, the data for (ii) and (iii) (dashed and dotted lines) overlap one another, implying that adatom detachment is not so important as to influence the monomer and island densities. This is expected because, at low temperature, the thermal activation energy is so small that adatom detachment may not be operative. However, at relatively high temperature, i.e., at $T=300$ K, the deviation of the two curves is appreciable for both N_1 and N, implying that adatom detachment significantly affects the island density. Such differences may possibly alter the scaling behavior of the island density versus the deposition flux.

The influence of dimer mobility alone is not as simple as that of the detachment of adatoms. At a very early stage of the deposition, the deviation of the lines is not significant. This is because the dimers will rarely encounter an island in the low-coverage regime. However, as the coverage increases, the diffusing dimers readily encounter islands and aggregate with them or yield coalescence of two or more islands, resulting in a decrease in N even at the low temperature of $T=240$ K. A close look enables one to observe the difference between the plots for the two models (i) and (ii) (solid and dashed lines) in Fig. 2. Such an influence is even more pronounced at high temperature, i.e., at $T=300$ K, where dimers diffuse sufficiently rapidly to encounter the existing islands before dissociation takes place. On the other hand, if detachment of adatoms from the island edges is allowed, the island density is found to decrease more significantly whereas the monomer density increases.

The dynamical behavior of N_1 and N can be divided into four regimes, as in previous work:[11,12,22] a low-coverage regime (marked as L) corresponding to increasing monomer and island densities, an intermediate regime (I) in which the monomer density decreases while the island density still increases, an aggregation regime (A) in which the island density is nearly constant, and a coalescence regime (C) where the island density sharply decreases due to coalescence. In the early stage of growth, i.e., in the low-coverage regime, the monomer and island densities are found to increase following a power law as $N_1\sim\theta^{0.94}$ and $N\sim\theta^{2.6}$. The power for the island density is slightly smaller than that predicted by the rate equation. Since the island density in the early stage of deposition, obtained without small-cluster mobility, is known to agree fairly well with the rate equation prediction, we believe that the discrepancy is due to small-cluster mobility. In the aggregation regime, on the other hand, since the monomers and dimers aggregate with the existing islands, the size of islands increases in time, while the number of islands remains constant. Thus, the distribution of island size is self-similar in time and the dynamic scaling relation in Eq. (2) is expected to hold. Such a scaling relation will be discussed in detail below.

B. Monomer and island densities versus deposition flux

We calculate N_1, N_2, and N versus the deposition flux, for various values of the substrate temperature ranging from $T=180$ K to as high as $T=360$ K, for the models (ii) and (iii). The power-law behavior of N enables us to test whether or not the scaling relation in Eq. (3) holds before the onset of $i=2$ behavior, for which $\chi=\frac{1}{2}$ is expected.

Figure 3 shows N at the fixed coverage of $\theta=0.15$ ML versus deposition flux, obtained from the models (ii) (upper plot) and (iii) (lower plot), described earlier in this section. Since clusters of size larger than 1 cannot dissociate in (ii), the island density is defined as $N=\Sigma_{s\geqslant 2}N_s$. At low temperature, i.e., at $T=180$ K, the slope of the plot is $\chi\simeq 0.33$ (not shown), which is about 10% larger than that in earlier work by Liu, Bonig, and Metiu[15] and Bartelt *et al.*[16] We believe that this discrepancy is due to the excluded-volume effects of adatoms. In the earlier work, two atoms on the same site are assumed to form a dimer, whereas, in the present model, two atoms on neighboring sites are assumed to form a dimer. Thus, the island density obtained in the earlier work must have been underestimated by neglecting the nucleation events occurring between two monomers on neighboring sites. Our result is, however, consistent with $\chi=i/(i+2)$ for $i=1$, implying that the dimer mobility is indeed unimportant at low temperature, as we expect. It should be noted that the exponent χ would be $\chi=2i/(d+d_f+2i)\simeq 0.35$ (for $d_f=1.7$ and $i=1$) if the islands grew fractally; however, since D/F is small at low temperature, the islands do not appear to yield fractal structure, as we can see from the morphology in Fig. 1. As the substrate temperature increases, the slope increases. For $T=240$ K, the estimate is $\chi\simeq 0.37$ and, at sufficiently high temperatures such as $T\geqslant 280$ K, the estimate of χ is nearly constant and close to 0.39. Although this value is slightly smaller than that predicted by the scaling relation in

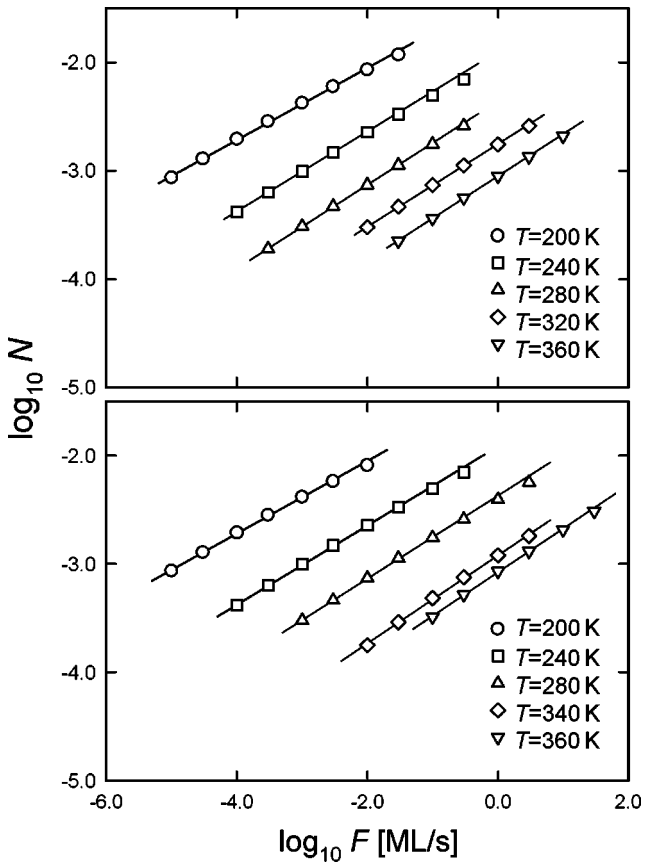

FIG. 3. The island density versus deposition flux on a log-log plot for various values of the substrate temperature. The upper plot is the simulation data for model (ii) and the lower plot for (iii).

Eq. (3), we believe it to be a good indication of the existence of the scaling regime of Eq. (3). It should be noted, however, that our estimate is larger by about 10% than that given in Ref. 15, presumably for the same reason as discussed before.

We also carried out additional simulations allowing both dimer mobility and trimer mobility but without allowing detachment, and obtained results basically similar to those presented in the upper plot of Fig. 3, suggesting that inclusion of the dimer mobility alone is sufficient to investigate the influence of small-cluster mobility (see Fig. 4).

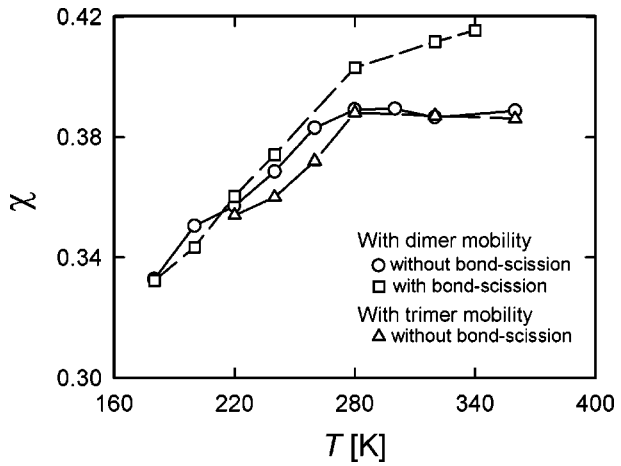

FIG. 4. Estimates of the scaling power χ for various values of the substrate temperature, for three different models of simulation.

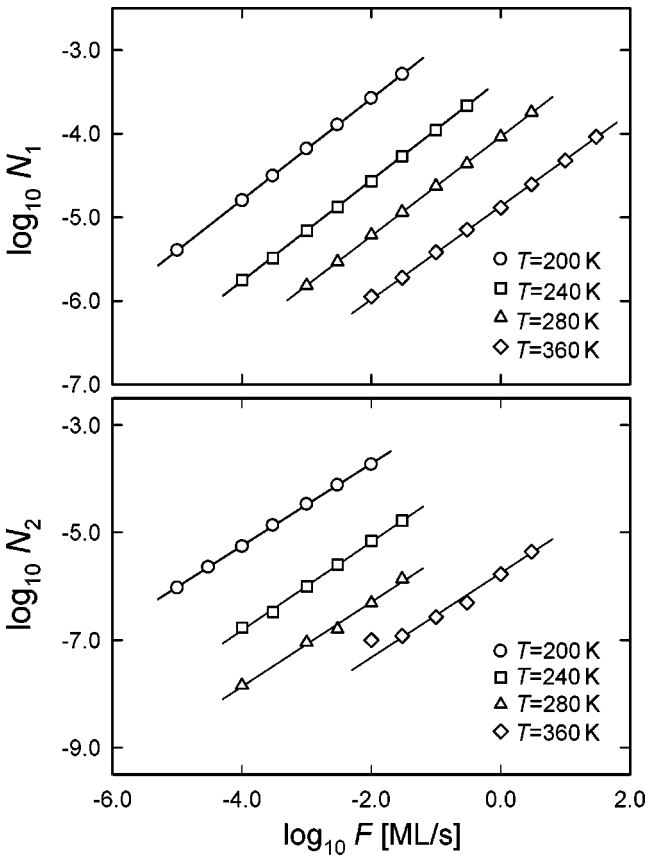

FIG. 5. The monomer density (top) and dimer density (bottom) plotted on a log-log scale for various values of the substrate temperature, obtained for model (iii).

In the lower plot of Fig. 3, since each dimer may be dissociated into two monomers, the island density is given as $N=\Sigma_{s\geqslant 3}N_s$. (Note that dimers are not considered to be stable islands in this case; however, we find that inclusion of dimers in the calculation of N does not affect the result appreciably.) At low temperature, i.e., at $T=180$ K, the slope was estimated to be close to $\frac{1}{3}$. This implies that monomer diffusion dominates dimer diffusion and adatom detachment, as we expect at low temperature. As the substrate temperature increases, such as for $T=240$ K and $T=280$ K, the estimates of the slope increase. For $T\geqslant 280$ K, the estimate of χ is continuously increasing beyond 0.4, unlike the case for (ii), though the rate of increase becomes smaller, as shown in Fig. 4. This observation is apparently different from the analytical prediction of Eq. (3), suggesting that the scaling regime of Eq. (3) does not exist for model (iii). Since we allowed adatom detachment from the island edges, our Monte Carlo model is distinct from the analytical model from which the rate equation is derived, particularly at high temperature. In the rate equation analysis, once the nucleation or aggregation event occurs, adatoms are assumed not to be detached from the islands. Thus, we believe that a more elaborate theory is necessary to explain the present Monte Carlo data.

Figure 5 shows the monomer and dimer densities at $\theta=0.15$ ML plotted against the deposition flux; the upper plot is the monomer density and the lower plot the dimer density. The scaling exponents γ_m, defined by $N_m\sim F^{\gamma_m}$ for $m=1,2$, are calculated for various values of the substrate tem-

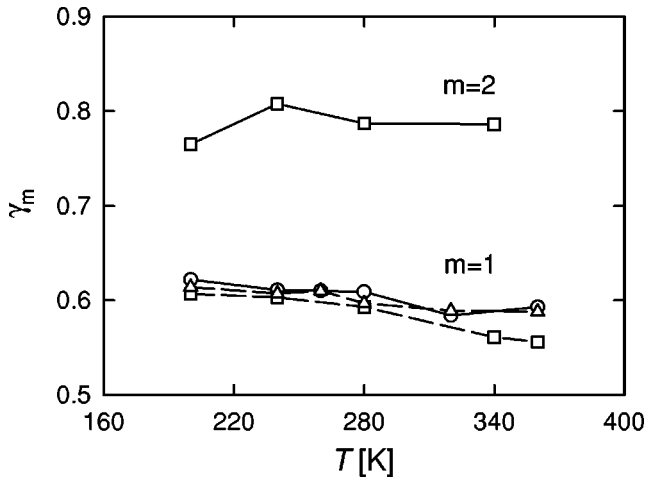

FIG. 6. Estimates of the scaling powers for the monomer and dimer densities, plotted against the substrate temperature. The symbols denote the data for the same simulation models as in Fig. 4.

perature and the results were plotted in Fig. 6. [Note that the dimer density was calculated only for model (iii) for which the detachment of adatoms is operative.] For the models without adatom detachment, the estimates of γ_1 for $T<280$ K are slightly larger than the rate equation prediction in Eq. (11), and, for $T\geqslant 280$ K, the results are nearly constant and close to $\frac{3}{5}$. This observation is consistent with the earlier observation for χ that the scaling relation derived by rate equation analysis is valid for $T\geqslant 280$ K. On the other hand, for the model with adatom detachment, the estimate of γ_1 decreases, though rather slowly, below $\frac{3}{5}$, implying that the agreement with Eq. (11) is poor. This is also consistent with the observation for χ that the intermediate scaling region may not exist for this model. It might be interesting to point out that the estimates of χ cross the convergence value of $\frac{2}{5}$ in the intermediate scaling region of Eq. (3) at a temperature of about 280 K, and, for this temperature, the estimates of both γ_1 and γ_2 are also similar to those predicted by Eqs. (11) and (12), i.e., $\gamma_1=\frac{3}{5}$ and $\gamma_2=\frac{4}{5}$, respectively. We believe that this consistency justifies our simulation data.

C. Scaling of the island size distribution

The dynamic scaling function defined in Eq. (2) is calculated for various models, with and without edge diffusion, small-cluster mobility, and adatom detachment, for selected values of the substrate temperature. In order to observe the influence of adatom diffusion along island edges, we plot in Fig. 7 the scaling function obtained (a) without edge diffusion and (b) with it, for $T=240$ K, $T=280$ K, and $T=336$ K and for $F=0.01$ ML/s. Detachment of adatoms from island edges and small-cluster mobility are not allowed for this purpose. At low temperature, since adatoms diffuse relatively short distances before nucleation takes place, the density of islands becomes large but the mean size of islands is small. The distribution of island size is expected to be self-similar in time, implying the dynamic scaling relation in Eq. (2) to hold. As the temperature increases, the island density becomes smaller whereas the mean island size increases. Indeed, scaling holds as we can see from Fig. 7(a); however, interestingly, the scaling functions for various temperatures

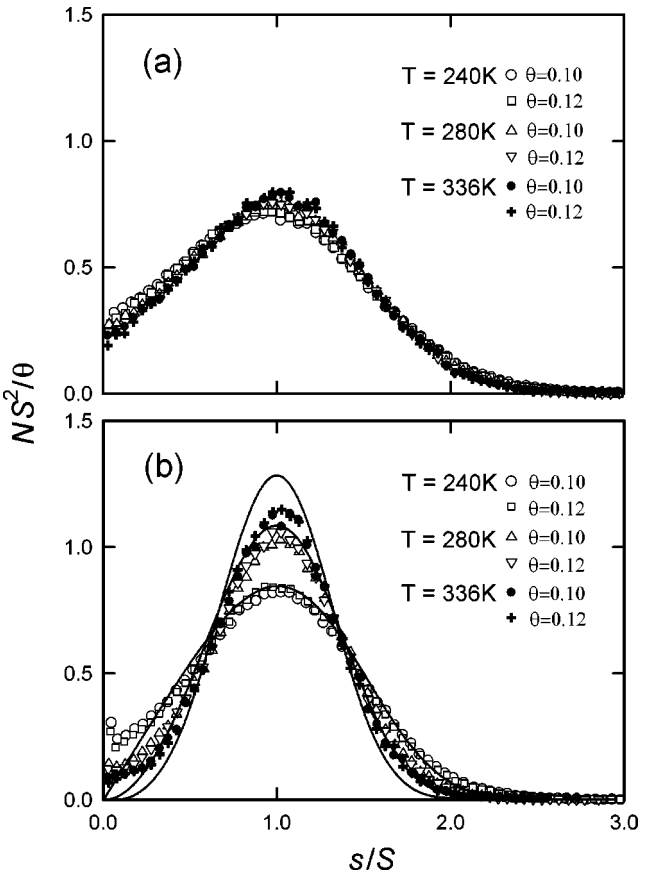

FIG. 7. The scaling function given in Eq. (2), obtained from simulations (a) without edge diffusion and (b) with edge diffusion, for selected values of the substrate temperature. Small-cluster mobility and detachment are not allowed in either case. The solid lines in (b) are the analytical predictions for the critical island size for (from bottom to top) $i=1$, $i=2$, and $i=3$.

are not appreciably different from each other within the range of temperature selected. It should be noted that the quality of data collapse for $T=240$ K is worse than in the other two cases. This is because dynamic scaling does not hold for small values of the diffusion-to-deposition ratio D/F, as is widely known. For $T=240$ K, the value of D/F is about 4×10^6, which is indeed small to expect the scaling relation to hold. For $T=280$ K and 336 K, on the other hand, the values of D/F are, respectively, 6.4×10^7 and 10^9, and the data show reasonably good collapse over the range of $\Delta\theta=0.1$ ML or even larger, depending on the cases, though we show the plots only for two typical values of θ in the middle of the aggregation regime. Similar concerns may be valid for all data in the subsequent discussion.

Edge diffusion, on the other hand, results in dramatic changes in the scaling function. It seems clear that edge diffusion not only yields a geometrical phase transition from fractal to compact islands, but also alters the scaling function. In Fig. 7(b) the symbols are the simulation data and the solid lines are the analytical results[11] for the scaling function for, from bottom to top, $i=1$, $i=2$, and $i=3$. For low temperature, i.e., for $T=240$ K, the scaling function is rather similar to that of the analytical prediction for $i=1$; however, as the temperature increases, the peak of the scaling function increases, indicating that the scaling function depends on the

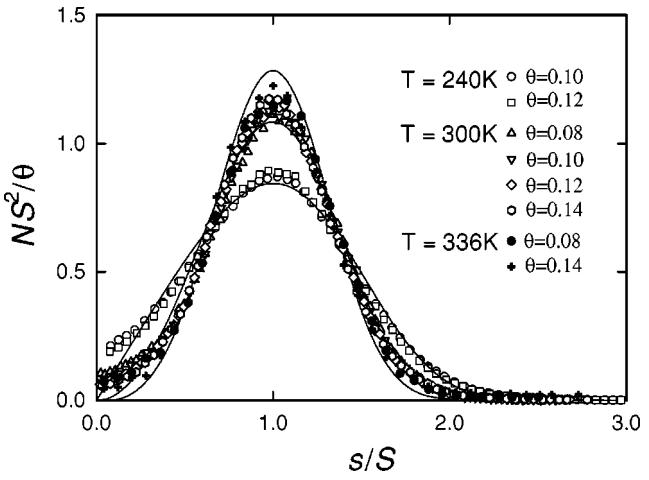

FIG. 8. The scaling function given in Eq. (2), obtained from simulations for case (ii), for selected values of the substrate temperature.

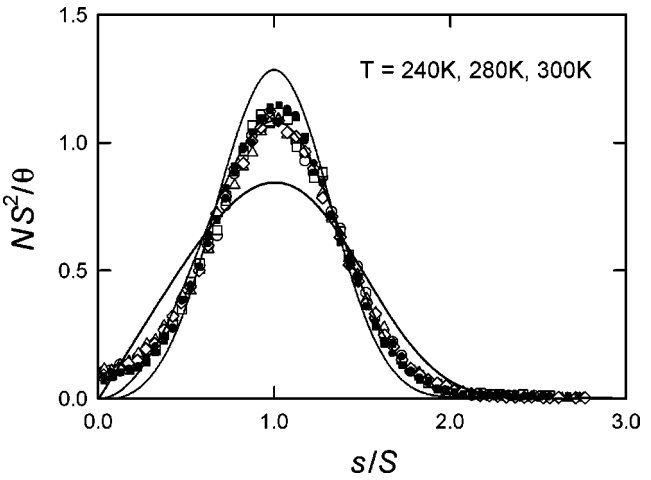

FIG. 9. The scaling function in Eq. (2), obtained from simulations for model (iii), for selected values of the substrate temperature and for $\theta=0.1$ and 0.12. Note that, since dimers can be dissociated into two monomers, the present model is similar to that for $i=2$.

temperature, unlike in the cases without the edge diffusion. The scaling function for $T=280$ K is similar to the analytical prediction for $i=2$, while that for $T=336$ K increases further, although it is smaller than that for $i=3$. This is rather surprising since the scaling function for compact islands is known to be similar to that for fractal islands.

We surmise that such variation of the scaling function is caused by small-cluster mobility due to edge diffusion. Consecutive slipping of adatoms along the island edges yields mobile small clusters such as dimers and trimers. Since the hopping rate of edge diffusion is given by $D_e = De^{-\Delta E_e/k_BT}$ ($\Delta E_e = E_e - E_{d1}$), it increases as the temperature increases more rapidly than the rate of surface diffusion and, accordingly, the mobility of small clusters by edge diffusion also increases. At low temperature, such small-cluster mobility is unimportant, yielding a scaling function similar to that for $i=1$, as we expect; however, as the temperature increases, edge diffusion appears to cause mobility of small clusters sufficiently large as to alter the scaling functions. The scaling region appears to be rather narrow, implying that the island morphology is self-similar only for a short period.

Plotted in Fig. 8 are the scaling functions obtained by allowing dimer mobility (but without adatom detachment), for $T=240$ K, $T=300$ K, and $T=360$ K. (Note that we plotted the data for a larger range of coverage compared with Fig. 7, to specify the domain of validity of self-similarity of the island morphology.) At relatively low temperature, $T=240$ K, since the dimers diffuse slowly, monomer diffusion dominates the dimer mobility and, therefore, the scaling function is similar to that for $i=1$; however, the scaling function is enhanced slightly by dimer mobility, compared with the corresponding data in Fig. 7(b). Thus it appears that the dimer mobility caused by consecutive edge diffusions is already sufficient to influence the scaling function. As the temperature increases, the rate of dimer hopping increases. For $T=300$ K, the scaling function is found to be rather close to (though slightly larger near the peak than) that for $i=2$ as shown in the figure, again implying that the mobility of dimers influences the scaling function. It is interesting that the scaling function is similar to (or even larger than) that for $i=2$, despite that the dissociation of dimers is disallowed. This is similar to the observation by Lee, Amar, and Family[22] from simulations of epitaxial growth of thin films with incompatible materials. In their work, the scaling function was found to vary as the rates of hopping-up and hopping-down processes increase. Such consecutive hopping-up and hopping-down processes are known to yield mobile dimers and trimers, and such small-cluster mobility was found to alter the scaling functions. It is interesting to see whether or not the scaling function varies like that for $i=3$ if the substrate temperature increases further. However, our data for $T=336$ K show that this is not the case, as shown in Fig. 8. The scaling function is not appreciably different from that for $T=300$ K and appears to converge to a certain limiting value.

Figure 9 shows the data when both dimer mobility and adatom detachment are allowed, for three different values of the substrate temperature. Since each dimer can be dissociated to two monomers, the present model is similar to that for $i=2$. (Note, however, that, since each trimer may be dissociated to a monomer and a dimer, our model is not rigorously the same as that for $i=2$.) Indeed, the scaling function is close to the analytical prediction for $i=2$. Data for various values of the temperature appear to collapse onto a single curve, suggesting that the scaling function is not sensitive to the substrate temperature, unlike the case without adatom detachment. Thus, both dimer mobility and adatom detachment affect the scaling function significantly over a wide range of temperature.

V. SUMMARY AND CONCLUSIONS

We have calculated monomer and island densities versus coverage and deposition flux for epitaxial growth of thin films with and without small-cluster mobility and detachment of adatoms, for various values of the substrate temperature. We found that the scaling power characterizing the island density versus the deposition flux increases as the substrate temperature increases. At low temperature, the scaling exponent χ was found to be close to $\frac{1}{3}$ for all models, which agrees with $\chi=i/(i+2)$ for $i=1$, suggesting that

monomer diffusion dominates small-cluster mobility and adatom detachment. As the temperature increases, the exponent increases. We found, at sufficiently high temperature, that the exponent obtained allowing dimer mobility but disallowing detachment of adatoms yielded a scaling regime in which mobility of small clusters has a non-negligible effect before the onset of $i=2$ behavior. On the other hand, on allowing adatom detachment, we found that the exponent appears to increase continuously beyond $\chi=\frac{2}{5}$. Thus, it seems clear that, in analyzing the experimental data, one should consider the scaling relation in Eq. (3) only when the dissociation barrier of adatoms is relatively large compared with the activation energy of small-cluster diffusion.

We also found that small-cluster mobility and adatom detachment influence the dynamic scaling functions. Assuming that dimers and trimers diffuse and adatoms may be detached from the island edges, we found that the scaling function is similar to the analytical prediction for $i=2$, independent of the temperature. We also found that dimer mobility alone (without detachment) alters the scaling function from $i=1$ behavior to $i=2$ behavior as the substrate temperature increases.

ACKNOWLEDGMENT

This work was financially supported by the Korea Science and Engineering Foundation under Grant No. KOSEF 981-0207-029-2.

[1] J. W. Matthews, *Epitaxial Growth* (Academic, New York, 1975).
[2] B. Lewis and J. C. Anderson, *Nucleation and Growth of Thin Films* (Academic, New York, 1978).
[3] J. Y. Tchao, *Materials Fundamentals of Molecular Beam Epitaxy* (World Scientific, Singapore, 1993).
[4] L. Bardotti, P. Jensen, A. Hoareau, M. Treilleux, and B. Cabaud, Phys. Rev. Lett. **74**, 4694 (1995).
[5] Z. Zhang, X. Chen, and M. G. Lagally, Phys. Rev. Lett. **73**, 1829 (1994).
[6] P. Jensen, A.-L. Barabasi, H. Larralde, S. Havlin, and H. E. Stanley, Phys. Rev. E **50**, 618 (1994).
[7] A. Venables, G. D. Spiller, and M. Hanbucken, Rep. Prog. Phys. **47**, 399 (1984); C. Ratsch, A. Zangwill, P. Smilauer, and D. D. Vvedensky, Phys. Rev. Lett. **72**, 3194 (1994); L.-H. Tang, J. Phys. (France) **3**, 935 (1993).
[8] M. Schroeder and D. E. Wolf, Phys. Rev. Lett. **74**, 2062 (1995); note that in their definition χ characterizes the mean distance between nucleation sites, and twice the inverse is equivalent to the current definition.
[9] F. Family and P. Meakin, Phys. Rev. Lett. **61**, 428 (1988); Phys. Rev. A **40**, 3836 (1989).
[10] W. W. Mullins, J. Appl. Phys. **59**, 1341 (1986).
[11] J. G. Amar, F. Family, and P.-M. Lam, Phys. Rev. B **50**, 8781 (1994).
[12] F. Family and J. G. Amar, Mater. Sci. Eng., B **30**, 149 (1995).
[13] M. C. Bartelt and J. W. Evans, Phys. Rev. B **46**, 12 675 (1992).
[14] J. G. Amar and F. Family, Phys. Rev. Lett. **74**, 2066 (1995).
[15] S. Liu, L. Bonig, and H. Metiu, Phys. Rev. B **52**, 2907 (1995).
[16] M. C. Bartelt, S. Gunther, E. Kopatzki, R. J. Behm, and J. W. Evans, Phys. Rev. B **53**, 4099 (1996).
[17] J. Villain, A. Pimpinelli, L. Tang, and D. Wolf, J. Phys. (France) **2**, 2107 (1992); J. Villain, A Pimpinelli, and D. Wolf, Comments Condens. Matter Phys. **16**, 1 (1992).
[18] J. Hoshen and R. Kopelman, Phys. Rev. B **14**, 3438 (1976).
[19] P. J. Feibelman, Phys. Rev. Lett. **58**, 2766 (1992).
[20] S. Liu, Z. Zhang, J. K. Norskov, and H. Metiu, Surf. Sci. **321**, 161 (1994).
[21] T. J. Raeker and A. E. DePristo, Surf. Sci. **317**, 283 (1994).
[22] S. B. Lee, J. G. Amar, and F. Family, Physica A **245**, 337 (1997).